Hot spots detection of solar cells based on visual saliency and nonsubsampled contourlet transform

Hot spots detection of solar cells based on visual saliency and nonsubsampled contourlet transform

L Y Dai[1], Q Y Zheng[1,2], H F Zhou[1,2], P J Lin[1], Z C Chen[1], L J Wu[1] and S Y Cheng[1]

[1]Institute of Micro/Nano Devices and Solar Cells, College of Physics and Information Engineering, Fuzhou University, Fuzhou 350116, China

E-mail: zhengqy@vip.sina.com/zhhafa@163.com

Abstract. Hot-spot effect is well-known in the practical application of solar cells. The faults of hot spots seriously affect the performance and service life of solar cells. In order to highlight the infrared and visible complementary information of hot spots and discover more details, this paper presents a novel method, which fuses an infrared image saliency map based on random rectangular regions of interest with visible image by NonSubsampled Contourlet Transform (NSCT). Firstly, the infrared hot spots image was detected by saliency map which is randomly sampled. Secondly, the infrared and visible image of the hot spots are transformed into high-frequency and low-frequency sub-bands by NSCT. Finally, absolute value maximization and saliency map guidance are used to fuse low-frequency and high-frequency sub-bands respectively. The experimental results demonstrate that, compared with a set of related fusion methods, the presented method can better highlight the hot spots and other abundant information in visibility. It achieves accurate defects locating ability and has better performance on subjective and objective quality evaluation.

1. Introduction

Solar cells play a vital role in solar power generation, which is a kind of new energy technology with immense potential. When the solar cells are shaded or damaged, the operating current exceeds the short-circuit current of the cells and then hot spots happen unexpectedly [1]. The hot-spot phenomenon reduces the service life and safety of the cells. Under normal circumstances, hot spots will cause defects in the appearance of cells, but the appearance of inspection does not completely find the hot spot failure. Statistics show that only 19% of the appearance of solar cells would appear visible defects when the cells exist hot-spot problems. Therefore, visible inspection can't be used as common solution for checking hot-spot defects. Besides inspecting by visible images, electroluminescence (EL) image and thermal infrared image have been widely used to find hot-spot failures. EL imaging is a non-destructive manner which is developed to detect electric charges under forward bias. For a normal EL image, the light intensity is proportional to the voltage while other electrically inactive sections are described as dark regions. EL inspection of photovoltaic (PV) modules can accurately indicate the presence and location of cell failures [2]. However, EL image might cause region classification error. In terms of infrared thermography, it is also a non-invasive approach to detect radiation and produce images of that radiation which is emitted by all objects with a temperature above absolute zero. Thermal infrared image processing and Canny edge detection operator are practically utilized for fault diagnosis in solar cells [3]. Although this method performs well in the detection of hot-spot faults in

large size, it does not work well in small-scale details.

As is known, infrared and visible image fusion is an important branch of multi-source image fusion [4]. It combines the target detection characteristics of infrared images with scene-keeping characteristics of visible images, which overcomes the strong dependence of a single visible image in the light conditions. And it surmounts the shortcomings of infrared images including low contrast and blurred background. In aspect of small-scale detection, image fusion conducts well rather than the method presented in [3]. Using image fusion approach to fuse infrared and visible images of hot spots can improve the recognition accuracy and duly locate faults for subsequent investigation. Human vision is able to quickly search for targets. If visual saliency is introduced into the infrared image of hot spots, the possible presence of hot spots can be quickly identified, thereby locating hot spots and greatly reducing background interference. A proposed Laplacian pyramid method is basically applied in spatial domain and determine target, which reduces the color distortion of the fused image [5]. Among the mentioned multi-scale transform (MST) approaches, a method proposed in [6] keeps more original information than the pixel level. Image fusion based on Curvelet Transform (CVT) presented in [7] preserves spectral characteristics. Due to the profitable properties of NonSubsampled Contourlet Transform (NSCT), Li *et al* used this transform for determining the properties to improve the quality of the fused image [8]. However, traditional image fusion by MST has some shortcomings. For instance, some details of the image can't be caught and fusion rules only rely on single feature. So an infrared image fusion algorithm based on visual saliency and contrast enhancement is proposed [9]. However, there are limitations in capturing directional information by proposed method in terms of diverse image fusion tasks. A new fusion algorithm for infrared and visible images by combining salient region detection with NSCT is presented in [10]. However, this method is short of universality in solar cells hot-spot detection.

Inspired by those methods above, to obtain a high-performance of infrared and visible image fusion, we present an efficient approach to pre-process infrared image which is based on random sampling of the image into rectangular regions of interest. Then, an improved NSCT method which is a shift-invariant, multi-scale, and multi-directional transform has applied to image fusion. It can capture significant solar cells hot-spot faults features along all directions.

The rest of this paper is organized as follows. In Section 2, the proposed method is descripted. In Section 3, a saliency map approach of infrared hot-spot image is presented. In Section 4, NSCT fusion algorithm based on saliency guidance is analysed. In Section 5, experimental results are discussed. Finally, conclusions are summarized in Section 6.

2. The proposed method

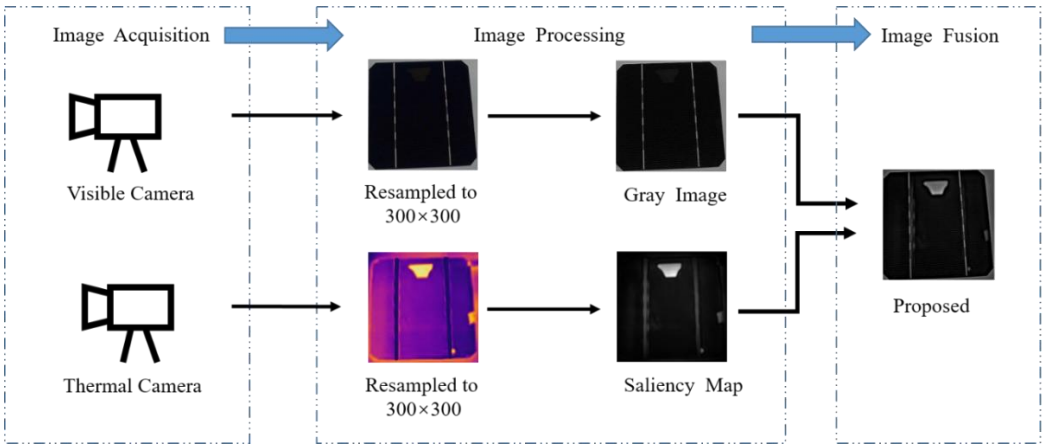

Figure 1. Image processing structure of proposed method.

The proposed method contains two main stages including visual saliency detection and NSCT. The goal of visual saliency detection is generating saliency map of infrared hot-spot image, while NSCT aims to combine information of multi-source image. Owing to shift-invariant and multi-scale properties of NSCT, this paper fuses an infrared saliency map, which samples random rectangular regions of interest of hot-spot, with the visible image by NSCT. The structure of our approach is shown in figure 1.

3. Visual saliency detection

In this section, to overcome local saliency, we propose a global saliency map which computes saliency map by randomly sampling rectangular regions. This method generates a great deal of random rectangles on regions of interest. Then the global saliency map is obtained by fusing all the local saliency maps acquired from these rectangles. As a result, stability has been greatly improved. The saliency map extraction process is shown in figure 2.

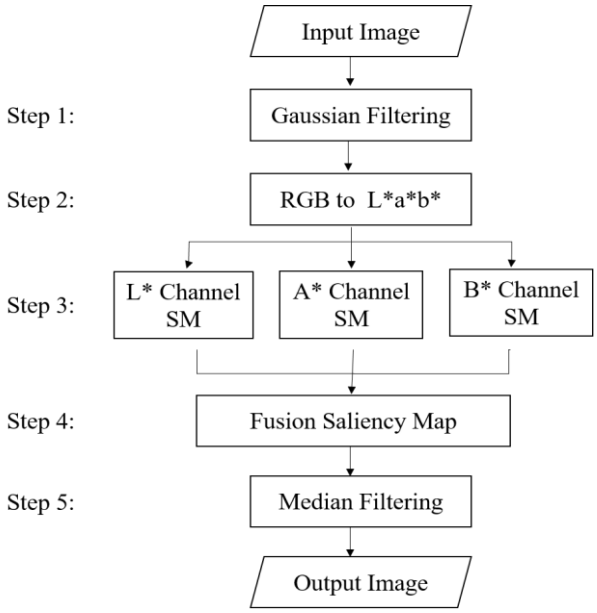

Figure 2. Saliency map extraction process.

The presented saliency map method includes five steps as follows:

- Step 1: To remove noise, an input infrared hot-spot image is initially applied to a Gaussian filter.
- Step 2: Performing CIE L*a*b* space conversion on filtered RGB image. Furthermore, the L*a*b* space is decomposed into L*, a*, b* channels respectively.
- Step 3: Randomly generating n sub-windows over each channel. In this paper, the proposed method set n as 800. For *k*th rectangular sub-window, Avg_k can be defined as ratio of the sum of grey values to rectangular area, as shown in formula (1). The saliency map value in each sub-window SM_k is denoted as the sum of the absolute value of difference between pixel intensity $I_k(i,j)$ and Avg_k of *k*th sub-windows. Finally, SM can be determined according to equation (3).

$$Avg_k = \frac{\sum_{i=x_{k1}}^{x_{k2}} \sum_{j=y_{k1}}^{y_{k2}} I_{i,j}}{(x_{k2} - x_{k1} + 1)(y_{k2} - y_{k1} + 1)} \tag{1}$$

$$SM_k = \sum_{i=x_{k1}}^{x_{k2}} \sum_{j=y_{k1}}^{y_{k2}} \left| I_k(i,j) - Avg_k \right| \tag{2}$$

$$SM = \sum_{k=1}^{n} SM_k \tag{3}$$

- Step 4: Computing saliency map by pixel-wise Euclidean norm, and integrating the saliency map together. SM represents the saliency map of fused image, where LM , AM , BM are saliency map value of L* channel, a* channel and b* channel respectively.

$$SM = \sqrt{LM^2 + AM^2 + BM^2} \tag{4}$$

- Step 5: In this paper, median filter is applied to distribute saliency map values.

The proposed method in this paper not only extracts the hot-spot target but also keeps the edge details while fully restrained the background information of the infrared image. Solar cells hot-spot salient extraction is shown in figure 3.

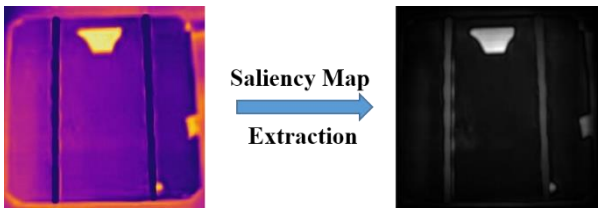

Figure 3. Image of solar cells hot-spot salient extraction.

4. NSCT based on saliency guidance

The NSCT is constructed by Non-Subsampled Pyramid Filter Bank (NSPFB) and Non-Subsampled Directional Filter Bank (NSDFB). On one hand, an NSDFB structure can detect information in fine directions and display the intricate directional structure well. On the other hand, an NSPFB can check information in multi-scale property [9]. Figure 4 shows the NSFB structure that implements the NSCT.This transform does not contain down-sampling or up-sampling on the decomposition of image, and the size of each sub-band image is the same as that of the source image, which ensures the shift-invariance of NSCT and reduces the spectrum aliasing and pseudo-Gibbs phenomenon [10].

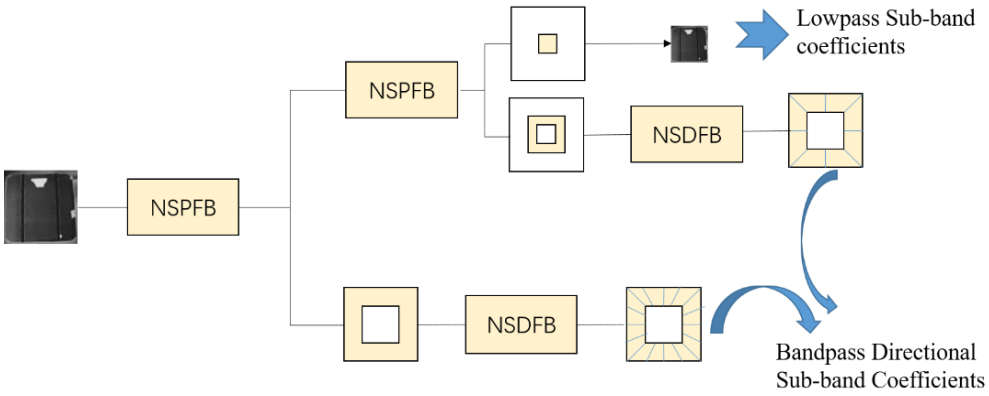

Figure 4. NSFB structure that implements the NSCT.

In this paper, a saliency map of hot-spot image is detected by a visual saliency detection method proposed above. then, the infrared and visible images are subjected to NSCT, respectively. Using the

saliency map of infrared images to guide the fusion of low-frequency sub-band coefficients, while high-frequency sub-band coefficients adopt absolute value maximization. Finally, the fused image is obtained through inverse transform of NSCT.

The proposed NSCT fusion rules contain two aspects shown as follows:

The sub-band coefficients of infrared and visible image via NSCT are defined as $C_{j_0}^{\text{ir}}(m,n)$, $C_{j_t}^{ir}(m,n)$ and $C_{j_0}^{\text{vis}}(m,n)$, $C_{j_t}^{vis}(m,n)$. Where, $C_{j_0}(m,n)$ is low-frequency sub-band coefficient, $C_{j_t}(m,n)$ is high-frequency sub-band coefficient, and $j_t > j_0$.

4.1. Low-frequency fusion rule

Low-frequency sub-band coefficients are guided by proposed saliency map in section 3. $C_{i,j}^{f,L}(m,n)$ denotes low-frequency sub-band coefficients of fused image.

$$C_{j_0}^{f}(m,n) = \omega_{\text{ir}}(m,n) * C_{j_0}^{\text{ir}}(m,n) + \omega_{\text{vis}}(m,n) * C_{j_0}^{\text{vis}}(m,n) \tag{5}$$

$$\omega_{\text{ir}}(m,n) + \omega_{\text{vis}}(m,n) = 1 \tag{6}$$

Where, $\omega_{\text{ir}}(m,n)$ is the value of infrared image saliency map *SM* normalized to [0, 1].

4.2. High-frequency fusion rule

While high-frequency sub-band coefficients of the image reflect the abrupt characteristics, such as edges or details. This method adopts absolute value maximization strategy. High-frequency sub-band coefficients of fused image $C_{j_t}^{f}(m,n)$ at location (m, n) is described as follows:

$$C_{j_t}^{f}(m,n) = \begin{cases} C_{j_t}^{ir}(m,n), \left|C_{j_t}^{ir}(m,n)\right| \geq \left|C_{j_t}^{vis}(m,n)\right| \\ C_{j_t}^{vis}(m,n), else \end{cases} \tag{7}$$

This method which consist of NSCT and saliency map helps to identify the hot-spot faults. It analyses the faults texture to detect the most distinctive characteristics.

5. Experimental results

In order to verify the fusion performance of this proposed method and reduce the error caused by pre-processing, strictly registered images are employed in this paper. The proposed method is compared with other five image fusion algorithms, including Laplacian pyramid(LP), dual-tree complex wavelet transform(DTCWT), curvelet transform(CVT), nonsubsampled contourlet transform (NSCT) and CVT improved by proposed saliency map(SM-CVT).

5.1. The design of experiments

So far, there are few public image libraries used for hot-spot detection. We establish a test image library referring to the method of [11]. The ambient temperature should be taken into account in the experiments. In order to reduce the differences among built images, the experiments should be carried out in isothermal environment around 25°C. A test image library containing 100 images of solar cells hot-spot faults is constructed. There are three kinds of images. 40 images contain single-point faults. Another 40 images contain mass faults. The rest of images contain both single-point and mass faults.

5.2. Subjective evaluation

In order to detect single-point and mass faults, this paper selects images containing both types of faults from the test image library. The circular areas are single-point faults, while the rectangular areas are mass faults. As shown in figure 5, the LP, DTCWT, CVT and NSCT roughly fuse hot-spot target of infrared images, and the redundant grid lines extracted from visible background is obvious. As for

SM-CVT, the redundant grid lines can be removed, but the hot-spot target is blurred. As can be seen from figure 5(g), compared with the previous four methods, single-point and mass fault in the lower right corner of image is rather smaller. We develop a new image fusion method including visual saliency detection and NSCT. As shown in figure 5(h), this method not only highlights the hot-spot target, but also removes redundant grid lines. It can be concluded that this proposed method contains more details from source image and it has excellent intuitive judgment.

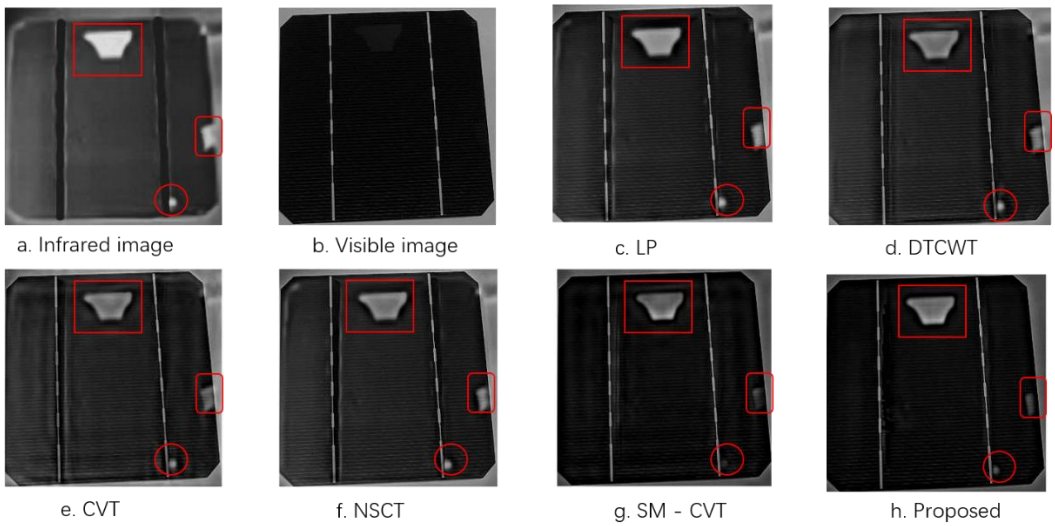

Figure 5. Subjective performance of various fusion methods.

5.3. Objective evaluation

In some cases, the subjective quality evaluation is time-consuming and influenced by the observer. To further evaluate quantitative performances of different fusion methods, we use four quality metrics, including Mutual Information metric *MI*, structural similarity based metric *SSIM*, Peak Signal to Noise Ratio metric *PSNR* and Root Mean Square Error metric *RMSE*, which have been proved to be effective to a certain extent. The metric *MI* reflects the degree to which the fusion result maintains the original image information. The metric *SSIM* is used to evaluate the structural similarity of structural signals. The metric *PSNR* can measure the noise in the fusion image. The metric *RMSE* shows the differences between the fusion image and the source image. For the first three metrics, a larger value indicates a better fused result. On the contrary, a smaller value of the metric *RMSE* corresponds to a better fused result.

Table 1. Objective performance of various fusion methods. The symbols '*MI*,' *SSIM*,' *PSNR*' and '*RMSE*' denote Mutual Information, Structural Similarity, Peak Signal to Noise Ratio and Root Mean Square Error, respectively.

Methods	*MI*	*SSIM*	*PSNR*	*RMSE*
LP	0.6356	0.5854	17.0659	0.0478
DTCWT	0.6002	0.5832	17.8612	0.1371
CVT	0.5943	0.5689	17.7414	0.0470
NSCT	0.6294	0.5746	17.6475	0.0470
SM-CVT	0.7525	0.8105	19.5951	0.0195
Proposed	**0.8236**	**0.8378**	**19.7128**	**0.0155**

Table 1 presents the quantitative comparison of experimental images above. From this table, the proposed method has the best fusion performance, and all the metrics are better than other algorithms.

It can be found that the proposed method detects hot-spot accurately, at the same time, it has better performance on subjective and objective quality evaluation as well.

6. Conclusions

In this paper, we propose a salient region detection random rectangular ROIs by sampling infrared distinctiveness and NSCT solar cells hot-spot detection method. Based on human bionics, the visual attention mechanism of human eyes is introduced into solar cell hot-spot detection in proposed method. The infrared target is enhanced, while background is restrained by sampling random rectangular regions of interest. According to the shift- invariance of NSCT, a strategy which uses the significance of infrared image to guide the fusion of low frequency sub-band coefficients is proposed. The experimental results show that the fusion image obtained by this method not only highlights the target information in the infrared hot-spot image, but also retains rich visible background which fully reflects the target and its scene information. The presented method performs well in subjective and objective evaluation, image fusion and hot-spot detection. However, there still exist several challenges resulting from time computational complexity and difficulty of image registration. Therefore, it is worthwhile reducing code redundancy and strictly implementing solar cells hot-spot image registration in further investigation. It is also envisaged to exploit the proposed method to locate a salient hot-spot region and design concise graphical user interface.

References

[1] Simon M and Meyer E L 2010 Detection and analysis of hot-spot formation in solar cells *Sol Energ Mat Sol C* **94** 106-13
[2] Tsanakas J A, Long H and Buerhop C 2016 Faults and infrared thermographic diagnosis in operating c-Si photovoltaic modules: A review of research and future challenges *Renew Sust Energ Rev* **62** 695-709
[3] Tsanakas J A, Chrysostomou D, Botsaris P N and Gasteratos A 2015 Fault diagnosis of photovoltaic modules through image processing and Canny edge detection on field thermographic measurements *International Journal of Sustainable Energy* **34** 351-72
[4] Ma J, Ma Y and Li C 2018 Infrared and visible image fusion methods and applications: A survey *Inform Fusion* **45** 153-78
[5] Sun J, Han Q, Kou L, Zhang L, Zhang K and Jin Z 2018 Multi-focus image fusion algorithm based on Laplacian pyramids *JOSA A* **35** 480-90
[6] Sahu V and Sharma G 2015 A hybrid approach of image fusion using modified DTCWT with high boost filter technique *International Journal of Computer Applications* **117** 22-7
[7] Wu Z, Huang Y and Zhang K 2018 Remote sensing image fusion method based on PCA and curvelet transform *J Indian Soc Remote* **3** 1-9
[8] Li L, Si Y and Jia Z 2017 Remote sensing image enhancement based on adaptive thresholding in NSCT domain *International Conference on Image, Vision and Computing IEEE* (Lucknow, India, 26 March, 2017) pp 319-22
[9] Zhou Y, Geng A, Wang Y, Chen J and Zhang Q 2014 Contrast enhanced fusion of infrared and visible images *Chinese Journal of Lasers* **41** 223-9
[10] Meng F, Song M, Guo B, Shi R and Shan D 2016 Image fusion based on object region detection and Non-Subsampled Contourlet Transform *Comput Electr Eng* **62** 375-83
[11] Tsai D M, Li G N, Li W C and Chiu W Y 2015 Defect detection in multi-crystal solar cells using clustering with uniformity measures *Adv Eng Inform* **29** 419-30